THE ASTROPHYSICAL JOURNAL, 355: L19–L22, 1990 May 20

VLA IMAGING OF EXTRAGALACTIC AMMONIA: HOT GAS IN THE NUCLEUS OF IC 342

PAUL T. P. HO
Harvard-Smithsonian Center for Astrophysics

ROBERT N. MARTIN
Steward Observatory

JEAN L. TURNER
University of California, Los Angeles

AND

JAMES M. JACKSON
Max-Planck-Institut für Extraterrestrische Physik

Received 1989 October 27; accepted 1990 February 26

ABSTRACT

Extragalactic NH_3 is successfully imaged with 5″ resolution using the VLA. Essentially all the single-dish flux is recovered in the interferometer maps. The hot gas ($\gtrsim 70$ K), inferred from single-dish NH_3 line intensity ratios, appears to be closely associated with the innermost portions of the nuclear bar seen in CO. Small-scale anticorrelation of the NH_3 emission with the central thermal radio continuum emission is likely to be due to heating and photoionization effects.

Subject headings: galaxies: nuclei — interstellar: molecules — radio sources: spectra

I. INTRODUCTION

Extragalactic ammonia was first detected in the $(J, K) = (1, 1)$ inversion line toward the nearby spirals IC 342 and NGC 253 (Martin and Ho 1979). This was followed by detection of the (2, 2) line (Martin, Ho, and Ruf 1982), as well as the (3, 3), (4, 4), and (6, 6) lines toward IC 342 (Martin and Ho 1986). The relative line intensities of all five transitions showed that the rotational states can be characterized by a common rotational temperature of ~ 50 K, suggesting a high gas temperature, ~ 70 K. High gas temperatures are not unexpected in the nuclei of galaxies since vigorous star formation is often indicated by radio continuum and infrared observations (e.g., Becklin *et al.* 1980; Turner and Ho 1983). However, CO maps of these regions, even with a resolution of several arcseconds (e.g., Lo *et al.* 1984), indicate low observed brightness temperatures ($\lesssim 10$ K). Since CO is likely to be thermalized, either beam dilution is important or CO traces only the cooler gas. Multitransitional NH_3 studies circumvent the beam dilution problem by taking line ratios (see Ho and Townes 1983). The success of the NH_3 transitions as good indicators of temperature has been demonstrated in Galactic studies (e.g., Mauersberger *et al.* 1986; Torrelles *et al.* 1986). Multitransitional studies are possible in other molecules. Recent CO $J = 3 \rightarrow 2$ and $J = 2 \rightarrow 1$ studies of IC 342 (Ho, Turner, and Martin 1987; Eckart *et al.* 1990) support the presence of hot ($\gtrsim 40$ K) gas in the nuclear region.

Since a hot gas component has been detected in IC 342, we are now interested in defining its location, spatial morphology, and dynamics. Various CO observations (Lo *et al.* 1984; Eckart *et al.* 1990; Ishizuki *et al.* 1990), which delineate the cooler gas, suggest the presence of a molecular gas bar as well as a ringlike structure in the nucleus. The question is whether the hot gas is associated with these CO structures or others detected in the radio continuum. An early attempt at using the VLA to study the NH_3 emission resulted in upper limits of 8 mJy or a brightness temperature of 0.5 K referred to 6″ resolution (Ho and Martin 1983). This led to the conclusion that the NH_3 emission, which was detected with 40″ resolution, must be extended over at least 18″ (390 pc at 4.5 Mpc; note that McCall 1989 suggests a much closer distance of 1.8 Mpc). Here we report the successful imaging, on our second attempt, of the NH_3 emission in IC 342 with the VLA. We find that the hot gas is intimately associated with the CO structures. Furthermore, in a comparison with the radio continuum emission, we conclude that the likely source of heating of the NH_3 gas is star-formation activity.

II. OBSERVATIONS

Aperture synthesis observations of the NH_3 emission were made with the Very Large Array (VLA) of the National Radio Astronomy Observatory,[1] near Socorro, New Mexico, during 1988 July 18 and 19. The antennas were in the D configuration, with a maximum baseline of 1 km. A total of ~ 15 hr of array time was used. The $(J, K) = (1, 1)$ and (2, 2) inversion lines of NH_3 were observed simultaneously by processing two independent intermediate frequencies. A total bandwidth of 25 MHz divided into 16 spectral channels was used to cover each frequency centered at $V_{LSR} = 50$ km s^{-1}. The resulting spectral resolution was 1.56 MHz, or ~ 19.7 km s^{-1}. Flux calibration was referred to 3C 286 with an assumed flux of 2.42 Jy at the observed frequencies. The passband calibrator was 3C 84 (measured flux of 39 ± 1 Jy), and the phase calibrator was NRAO 140 (measured flux of 2.7 ± 0.1 Jy). Absolute calibration at 1.3 cm wavelength is quite uncertain, especially during the summer months at the VLA. We estimate the uncertainty in flux densities to be of order 30%. We estimate the uncertainty in absolute position to be $\pm 0\farcs5$ based on phase noise.

[1] The National Radio Astronomy Observatory is operated by Associated Universities, Inc., under cooperative agreement with the National Science Foundation.

To produce the spectral line maps, we used natural weighting of the visibility data while applying a Gaussian taper of 50 kλ or 0.65 km (half-width at 30%). The resulting angular resolution is 5".1 × 4".7. This particular combination yielded the best signal-to-noise ratio. The velocity ranges −59 to 20 km s^{-1} and 80 to 159 km s^{-1} were judged to be free of line emission and were averaged to produce the continuum map that was subtracted from every spectral channel. Because of the low signal-to-noise ratio, neither self-calibration of the data nor CLEANing of the maps was attempted. When the resulting (1, 1) and (2, 2) line maps were examined, we found that differences between the two lines were not significant at the achieved sensitivity. We therefore averaged the (1, 1) and (2, 2) maps. This is reasonable since single-dish results (e.g., Martin and Ho 1986) indicate that the two lines are roughly equal in intensity.

Finally, to produce the maps displayed in Figure 1, we Hanning-smoothed the averaged (1, 1) and (2, 2) maps, reducing our velocity resolution to ~40 km s^{-1}. It is clear from Figure 1 that we have indeed detected extragalactic NH_3. Emission appears in the central three channels while it is absent in the adjacent channels used in the continuum subtraction. The emission is spatially extended, elongated north-south, ~30" × 10". Although the spectral channels are not completely independent, perceptible differences in emission structures with velocity are consistent with the observed CO velocity structure. To pursue this hypothesis further, we have calculated the zeroth and first moments for the emission (see Fig. 2). Isolated noise is suppressed in calculating the moments by clipping signals below a threshold of 1.5 mJy when the resolution of the maps is reduced to 40 km s^{-1} and 10" during the clipping procedure. This has the effect of emphasizing signals that are extended both spatially and in velocity.

For the integrated NH_3 emission, we find that two "arms" extend from the nuclear region. A comparison with the line-free continuum emission indicates that the NH_3 "arms" are associated with weak extensions in the radio continuum emission. Otherwise, the NH_3 and the continuum emission are anticorrelated in the sense that in the central region, where the radio continuum emission is strongest, the NH_3 emission is weakest. For the intensity-weighted velocity map, we find that the emission is extended in velocity with a south-north gradient increasing from 30 to 70 km s^{-1}. The detected gradient does not appear to be smooth or linear, but this conclusion is very much limited by the achieved sensitivity.

The total integrated NH_3 flux in the central 40" is ~990 mJy km s^{-1}. This is essentially 100% of the total flux, ~1000 ± 100 mJy km s^{-1}, detected on the Bonn 100 m telescope with 40" resolution (Martin and Ho 1986). The hot gas, inferred to be ~70 K from NH_3 line intensity ratios, is therefore likely to be distributed in armlike structures as in Figures 1 and 2. Within the 2' primary beam of the VLA antennas (Fig. 1), there are possibly other emission features with total integrated flux of

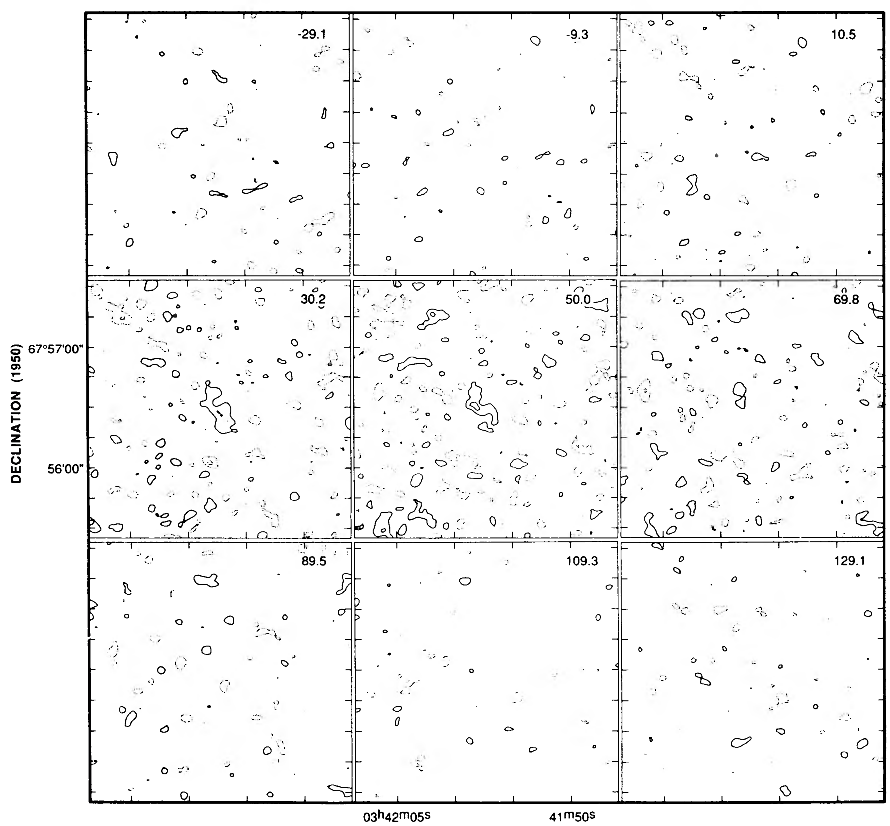

FIG. 1.—Extragalactic NH_3 emission in IC 342 as a function of velocity. The presented maps are an average of the (1, 1) and (2, 2) emission maps. The contour intervals in flux densities are −2, −1, 1, and 2 times 0.8 mJy beam^{-1}. The synthesized beam width is 5".1 × 4".7, PA −89°. The contour levels in brightness temperatures are therefore in steps of 0.16 K. The maps have been Hanning-smoothed in the spectral domain so that individual velocity channels are not independent. Note that the reality of the detected emission at 30 and 50 km s^{-1} rests on the extended nature of the emission, >30" × 10", well resolved by the synthesized beam.

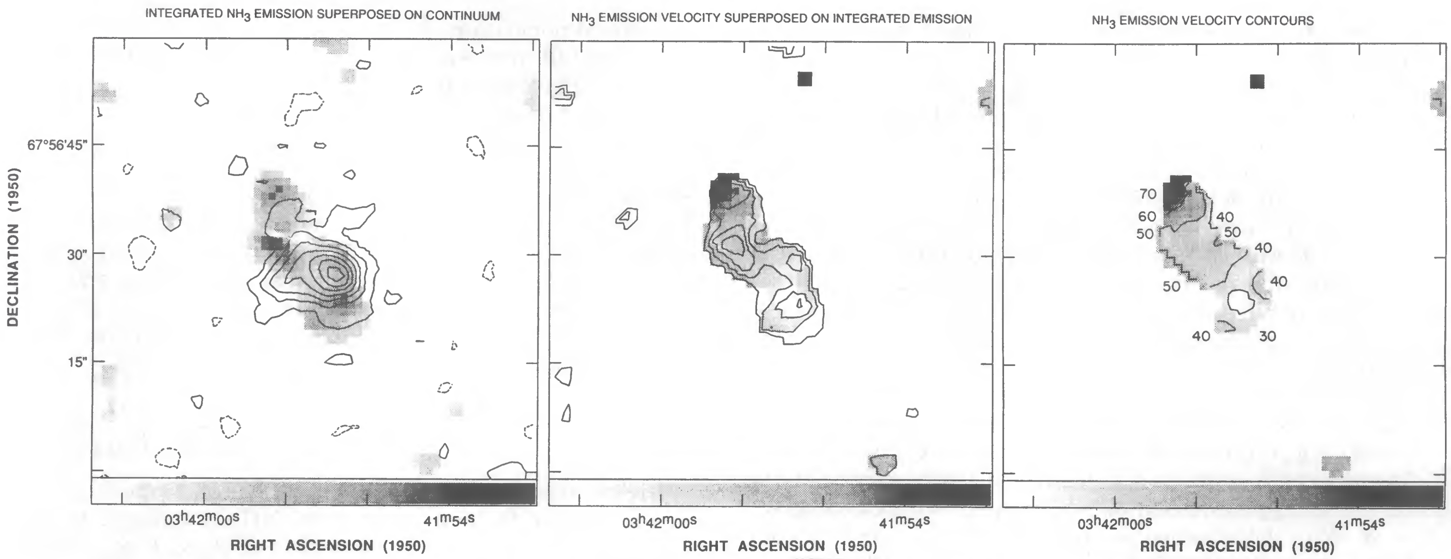

FIG. 2.—*Left:* Integrated NH_3 emission in IC 342 in gray scale, as compared to the 1.3 cm radio continuum in contours. The gray scale is linear from 0 to 250 mJy beam^{-1} km s^{-1}. The contour levels are -2, -1, 1, 2, 3, 4, 5, 6, and 7 times 1 mJy beam^{-1}. The synthesized beam width for the NH_3 emission is as in Fig. 1 and is 3″9 × 3″6, PA 85°, for the continuum emission. Note that there are noticeable extensions in the radio continuum emission in the directions of the NH_3 emission "arms." *Center:* The NH_3 emission velocity, calculated as a first-order moment, in gray scale superposed on the integrated emission in contours. The gray scale is linear from 30 to 70 km s^{-1}. The contour levels are -1, 1, 2, 3, 4, and 5 times 46 mJy beam^{-1} km s^{-1}. *Right:* The NH_3 emmission velocity in gray scale superposed on the isovelocity contours. The gray scale is again linear from 30 to 70 km s^{-1}, and the velocity contours are as labeled in km s^{-1}.

~500 mJy km s^{-1}. This may account for the increased noise levels in the central channels. However, we will not discuss further these features until better sensitivity is achieved.

The success of the current experiment can be traced to the improved *K*-band receivers and the increased processing capabilities of the correlator at the VLA. With roughly the same amount of actual integration time (but half the previous array time because of dual line operations), we achieved a noise level that is more than twice as sensitive as before. This is still a factor of 2 from theoretical sensitivity with the new *K*-band receivers, whose system temperatures are ~150 K at band center. We attribute the degraded performance in this experiment to summer weather and the fact that only 2/3 of the receivers had been upgraded at the time of the observations. In optimum winter conditions with all new *K*-band receivers, much better sensitivities should be possible.

III. DISCUSSION

a) The Central Molecular Bar in IC 342

The presence of a central molecular gas bar in IC 342 was first shown by the 7″ $J = 1 \rightarrow 0$ CO interferometer map of Lo *et al.* (1984). Other nuclear gas bars have since been found with CO interferometry in NGC 6946 (Ball *et al.* 1985), NGC 253 (Canzian, Mundy, and Scoville 1988), and Maffei 2 (Ishiguro *et al.* 1989). Single-dish observations of IC 342 in the $J = 2 \rightarrow 1$ and $J = 1 \rightarrow 0$ CO lines with 14″ and 21″ resolution, respectively, confirm the presence of the elongated central gas bar (Eckart *et al.* 1990). Most recently, 2″5 resolution CO maps from Nobeyama (Ishizuki *et al.* 1990) have resolved the central bar into two armlike features that are displaced by ~9″ in the east-west direction from each other. Both arms or ridges are elongated north-south with a size of ~25″ × 4″. These arms end in the nuclear region in a ringlike structure, ~3″ in radius, surrounding the central continuum core. In Figure 3, we overlay the integrated NH_3 intensity map with the Nobeyama integrated CO intensity map. Noting that the NH_3 map has an angular resolution that is coarser by a factor of 2, we find the overall spatial agreement to be excellent. The NH_3 emission is localized to the inner parts of the CO arms. The absence of NH_3 emission at >10″ from the nucleus, where the NH_3 emission drops by more than a factor of 3 while the CO emission drops by less than 25%, is a significant effect. Primary beam attenuation, lack of short spacings, and sensitivity effects are not important in the observed difference in spatial extents

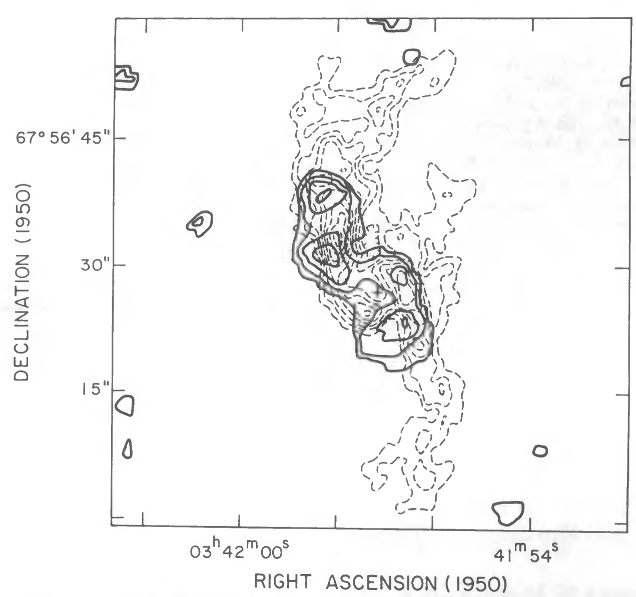

FIG. 3.—The integrated NH_3 emission map (*heavy contours*) is overlaid on the integrated CO emission map (*light contours*) from Ishizuki *et al.* (1990). The contour levels are evenly spaced and are 4.1 K km s^{-1} and 90 K km s^{-1} for the NH_3 and CO maps. Note that the primary beams are 2′ and 1′ for the NH_3 and CO maps, so that the absence of NH_3 emission toward the ends of the CO arms is significant and may be indicative of temperature effects.

between the two molecular species. The most likely explanation is heating effects via higher densities or higher temperatures. This is supported by the comparison to radio continuum emission (Fig. 2), where the NH_3 gas is closely associated with the predominantly thermal continuum emission (Turner and Ho 1983). We suggest that the CO emission traces the bulk of the molecular gas while the NH_3 emission traces the portions that are actively forming stars and are thus heated. The weaker NH_3 and CO emission toward the central continuum sources may be due to the ~ 10 times higher ionizing flux and the resultant heating. Either the central molecular gas is photoionized, or it is heated to such high temperatures that it radiates only weakly in the (1, 1) and (2, 2) lines. Molecular gas in the very center could also have been removed mechanically by shocks or winds as may be the case in M82 (e.g., Lo *et al.* 1987; Nakai *et al.* 1987; Carlstrom 1989). The lack of a ring structure in the NH_3 emission may be due to the poorer angular resolution as compared to the CO observations. With the achieved sensitivity, we cannot be very confident about these conjectures. When several NH_3 lines are imaged, their ratios will reveal the temperature distribution of the hot gas as well as its spatial morphology and variation.

b) *The Nature of the Hot Gas*

The peak brightness temperature of the NH_3 emission is ~ 0.35 K at 5″ resolution (~ 110 pc at 4.5 Mpc). If the gas is optically thick and thermalized to a gas temperature of ~ 70 K, the areal filling factor is on the order of 5×10^{-3}. Since the NH_3 emission is distributed over a large area, it is reasonable that within each synthesized beam, a large number of cloudlets or cores may exist. In the simplest model of n identical cloudlets with a typical size θ_s within the synthesized beam θ_b, we would have $n\theta_s^2/\theta_b^2 \sim 5 \times 10^{-3}$. Thus, $\theta_s \sim 8$ pc/$n^{1/2}$, so that for $\theta_s \sim 1$ pc, $n \sim 100$. This result is not very sensitive to the above assumption that the NH_3 gas is thermalized. The morphology of the NH_3 emission may well be a distributed population of hot molecular cloud cores surrounding young OB stars. Alternatively, the hot NH_3 emission could arise from the outer surfaces of molecular clouds that are externally heated by radiative or mechanical means (e.g., Stutzki *et al.* 1988; Jaffe *et al.* 1989). For a thermal radio continuum flux of ~ 1 mJy in a 4″ beam (Fig. 2), an ionizing flux of $\sim 10^{51}$ photons s^{-1} is required. This corresponds to ~ 150 O6 stars. Hence, the model of the NH_3 emission as embedded molecular cores seems quite reasonable. For the nearer distance of 1.8 Mpc (McCall 1989), both the number of cloudlets and the number of required O6 stars would decrease by a factor of 6.

We can estimate the amount of hot gas implied by the NH_3 measurements,

$$N_{NH_3} = 1.8 \times 10^{17}\ \mathrm{cm}^{-2} \left[\frac{J_\nu(T_{ex})}{70\ \mathrm{K}}\right]\left(\frac{\tau}{1}\right)\left(\frac{\Delta V}{40\ \mathrm{km\ s^{-1}}}\right)\left(\frac{f_{J,K}}{0.2}\right)^{-1},$$

where we assume a gas temperature of 70 K, an optical depth $\tau \sim 1$, and the fraction of the total NH_3 population in the detected rotational state to be $\sim 20\%$ at 70 K. If we further assume $(N_{NH_3}/N_{H_2}) \sim 10^{-7}$, we find a mass of $\sim 10^6\ M_\odot$ for the hot molecular component. This is in good agreement with the previous estimates of $\sim 10^6\ M_\odot$ based on $J = 3 \rightarrow 2$ CO measurements (Ho, Turner, and Martin 1987), although still with large uncertainties due to the assumed abundance ratio, the likely line opacity, and the distance.

Higher angular resolution observations of the hot gas may distinguish between the different models. For instance, the NH_3 emission appears to be somewhat shifted in position relative to the CO emission (Fig. 3). If this effect is real, peripheral heating may be the dominant mechanism rather than in situ star formation.

P. T. P. H. is supported in part by NSF grant AST87-20759. We thank our referee, Dan Jaffe, for a careful reading of our manuscript.

REFERENCES

Ball, R., Sargent, A. I., Scoville, N. Z., Lo, K. Y., and Scott, S. L. 1985, *Ap. J.* (*Letters*), **298**, L21.
Becklin, E. E., Gatley, I., Matthews, K., Neugebauer, G., Sellgren, K., Werner, M. W., and Wynn-Williams, C. G. 1980, *Ap. J.*, **236**, 441.
Canzian, B., Mundy, L. G., and Scoville, N. Z. 1988, *Ap. J.*, **333**, 157.
Carlstrom, J. 1989, Ph.D. thesis, University of California, Berkeley.
Eckart, A., Downes, D., Genzel, R., Harris, A. I., Jaffe, D. T., and Wild, W. 1990, *Ap. J.*, **348**, 434.
Ho, P. T. P., and Martin, R. N. 1983, *Ap. J.*, **272**, 484.
Ho, P. T. P., and Townes, C. H. 1983, *Ann. Rev. Astr. Ap.*, **21**, 239.
Ho, P. T. P., Turner, J. L., and Martin, R. N. 1987, *Ap. J.* (*Letters*), **322**, L67.
Ishiguro, M., *et al.* 1989, *Ap. J.*, **344**, 763.
Ishizuki, S., Kawabe, R., Ishiguro, M., Okumura, S. K., Morita, K.-I., Chikada, Y., and Kasaga, T. 1990, *Nature*, **344**, 224.
Jaffe, D. T., Genzel, R., Harris, A. I., Lugten, J. B., Stacey, G. J., and Stutzki, J. 1989, *Ap. J.*, **344**, 265.
Lo, K. Y., *et al.* 1984, *Ap. J.* (*Letters*), **282**, L59.
Lo, K. Y., Cheung, K. W., Masson, C. R., Phillips, T. G., Scott, S. L., and Woody, D. P. 1987, *Ap. J.*, **312**, 574.
Martin, R. N., and Ho, P. T. P. 1979, *Astr. Ap.*, **74**, L7.
———. 1986, *Ap. J.* (*Letters*), **308**, L7.
Martin, R. N., Ho, P. T. P., and Ruf, K. 1982, *Nature*, **296**, 632.
Mauersberger, R., Henkel, C., Wilson, T. L., and Walmsley, C. M. 1986, *Astr. Ap.*, **162**, 199.
McCall, M. L. 1989, *A.J.*, **97**, 1341.
Nakai, N., Hayashi, M., Handa, T., Sofue, Y., Hasegawa, T., and Sasaki, M. 1987, *Pub. Astr. Soc. Japan*, **39**, 685.
Stutzki, J., Stacey, G. J., Genzel, R., Harris, A. I., Jaffe, D. T., and Lugten, J. B. 1988, *Ap. J.*, **332**, 379.
Torrelles, J. M., Ho, P. T. P., Rodríguez, L. F., and Cantó, J. 1986, *Ap. J.*, **305**, 721.
Turner, J. L., and Ho, P. T. P. 1983, *Ap. J.* (*Letters*), **268**, L79.

PAUL T. P. HO: Harvard-Smithsonian Center for Astrophysics, 60 Garden Street, MS42, Cambridge, MA 02138

JAMES M. JACKSON: Max-Planck-Institut für Extraterrestrische Physik, Giessenbachstrasse, D-8046 Garching bei München, Federal Republic of Germany

ROBERT N. MARTIN: Steward Observatory, University of Arizona, Tucson, AZ 85721

JEAN L. TURNER: Department of Astronomy, UCLA, 405 Hilgard Avenue, Los Angeles, CA 90024